

## EFFECTS OF THERMAL ANNEALING AND PLASMA TREATMENT ON THE PROPERTIES OF ZNO

M. Rasulova

S. Zaynobidinov

Sh. Ermatov

L. Abdulfayizov

Andijan State University.

<https://doi.org/10.5281/zenodo.12589131>

**Abstract.** *This work presents a comparative study of the influence of thermal annealing and plasma treatment in hydrogen plasma on the properties of polycrystalline thin films of ZnO obtained by metalorganic chemical vapor deposition and obtained by the hydrothermal method*

**Key words:** *Sol-gel method, hydrodynamic conditions, surfactant, homogeneous, thermal annealing, plasma treatment.*

## ВЛИЯНИЕ ТЕРМИЧЕСКОГО ОТЖИГА И ПЛАЗМЕННОЙ ОБРАБОТКИ НА СВОЙСТВА ZNO

**Аннотация.** *В работе представлено сравнительное исследование влияния термического отжига и плазменной обработки в водородной плазме на свойства тонких поликристаллических пленок ZnO, полученных методом металлоорганического химического осаждения из газовой фазы и полученных гидротермальным методом.*

**Ключевые слова:** *золь-гель метод, гидродинамические условия, ПАВ, гомогенный, термический отжиг, плазменная обработка.*

Sol-gel technology is one of the common methods for producing ultrafine particles. Using this method, it is possible to obtain nanoparticles, porous structures with ordered and disordered pores, nanocoatings, fiber and monolithic structures, etc. The sol-gel method consists of two stages. At the first stage, a sol is synthesized, and then the resulting sol is converted into a gel [1].

Changing the pH of the reaction medium, varying the hydrodynamic conditions in which the sol is formed, controlling the viscosity of the reaction medium by selecting a solvent, choosing a surfactant, the composition of the reaction medium are the parameters on which the morphology of the resulting ultrafine zinc oxide particles depends. Works [2-3] show the influence of the pH of the reaction medium on the morphology of ultrafine zinc oxide particles. It was found that at a pH of 9, particles with sizes of 14 and 25 nm were obtained, and a further increase in pH leads to a decrease in the size of crystallites. In order to control the process of sol formation during synthesis, various structure-forming agents are used in addition to the sol former. In work [4], citric acid is used as a sol former, and ethylene glycol, polyethylene glycol and polyvinyl alcohol are used as structure-forming agents. It has been shown [5] that the morphology of zinc oxide nanoparticles is influenced not only by the nature of the structure-forming agent used, but also by its molar ratio with the sol former [5]. The advantages of the sol-gel method are: control of the structure of the final product at the stage of gel formation; elimination of numerous stages of washing sediments from interfering ions; obtaining a homogeneous product at the molecular level; high purity of the finished product. The disadvantages of the method are the production of agglomerated particles of zinc oxides and the need to use reagents based on salts of organic acids,

which are produced in limited quantities on the world market, which is unprofitable from an economic point of view. Recently, new promising directions for the synthesis of zinc oxide have been developed, based on the thermal decomposition of organic and inorganic salts. The main advantage of this production method is the possibility of synthesizing predominantly pure zinc oxide, and adjusting the parameters of the thermolysis process allows the formation of powders with a given dispersion and morphology. Salts are used as starting reagents in thermal decomposition processes, the anions of which can be easily removed during heat treatment: sulfates, carbonates, acetates, oxalates, nitrates, etc. However, the method of producing zinc oxide by thermolysis of inorganic compounds also has significant disadvantages, the main of which is the need recycling of gaseous products and the use of technological equipment made of corrosion-resistant materials. Therefore, it is advisable to use zinc carbonates, hydroxides or basic carbonates as starting compounds, which can be synthesized by the hydrothermal method.

Next, we will conduct comparative studies of the influence of thermal annealing and plasma treatment in hydrogen plasma on the properties of polycrystalline thin films of ZnO obtained by metal-organic chemical vapor deposition (MOCVD - ZnO) and obtained by the hydrothermal method (HT - ZnO). Two series of boron-doped ZnO films, n-type, were studied: I) films on glass substrates, synthesized by the MOCVD method at a temperature of  $\sim 200^{\circ}\text{C}$ , II) films on glass and crystalline silicon substrates, which were synthesized by the hydrothermal method (HT - ZnO) in real work. To obtain NT-ZnO samples, a thin ZnO seed layer was initially grown on a substrate by the sol-gel method. To prepare the seed layer, 0.4 g of zinc acetate  $\text{Zn}(\text{CH}_3\text{COO})_2 \cdot 2\text{H}_2\text{O}$  was dissolved in 10 ml of ethanol for 30 min at room temperature using a magnetic stirrer to obtain a homogeneous and transparent sol. Uniform distribution of the sol on the surface of the substrate was achieved by applying several drops to the substrate mounted on a horizontal table, followed by rotating the table at a speed of about 2000 rpm for 5 minutes. Final annealing at  $450^{\circ}\text{C}$  for 60 minutes in a muffle furnace resulted in the formation of a uniform seed layer. With continuous stirring, prepare an equimolar (0.3M) aqueous solution of zinc nitrate hexahydrate  $\text{Zn}(\text{NO}_3)_2 \cdot 6\text{H}_2\text{O}$  and hexamethylenetetramine  $(\text{CH}_2)_6\text{N}_4$ . Hydrothermal synthesis was carried out in a fluoroplastic beaker for 2 hours with stirring at  $90^{\circ}\text{C}$ . The samples were placed vertically, with the seed layer towards the wall of the glass. To obtain n-type ZnO films doped with boron, boric acid  $\text{H}_3\text{BO}_3$  was added to the solution at a concentration of 0.6 at.% to 3 at.%.

Aluminum nitrate  $\text{Al}(\text{NO}_3)_3 \cdot 9\text{H}_2\text{O}$  or aluminum chloride  $\text{AlCl}_3 \cdot 6\text{H}_2\text{O}$  from 0.6 at. % up to 3 atm. % was added to the solution to obtain n-type ZnO films doped with aluminum. After growth, the resulting samples were removed from the vessel, washed with distilled water in an ultrasonic bath for 10 minutes to remove residual particles adhering to the surface, and dried in an oven at  $100 - 110^{\circ}\text{C}$  for 5 minutes. The typical thickness of HT - Zn films doped with boron or aluminum after synthesis for 2 hours was  $0.8 - 1 \mu\text{m}$ , provided that the concentration of impurities in the solution was less than 1 at. %. Increasing the concentration of impurities in the solution led to slower growth. The samples were annealed in a quartz tube furnace. Annealing at atmospheric pressure was carried out in air or in a nitrogen flow with a purity of 99.999%. Annealing in a vacuum of  $\sim 2 \cdot 10^{-2}$  mbar was carried out during pumping with an oil rotary pump. Annealing in an oil-free vacuum of  $\sim 1 \cdot 10^{-5}$  mbar was carried out in an alundum furnace using a turbomolecular pump. Plasma treatment was carried out in a quartz reactor in a hydrogen

atmosphere at a pressure of 0.5 mbar with an RF power of 30 Wt (27.12 MHz). Measurements showed that during H – treatment for 5 minutes, the temperature of the samples increased to 50 – 70°C due to microwave absorption. The morphology of the samples was examined by scanning electron microscopy using a Quanta 200I 3D microscope (FEI). The crystal structure was studied using an MPD X-ray diffractometer. Optical transmission spectra in the range 190 – 1100 nm were measured with a Lambda spectrophotometer. Photoluminescence (PL) spectra were studied with a spectrophotometer in the wavelength range 300 – 850 nm when excited with a xenon flash lamp through a bandpass filter FF01 – 292/27 – 25 Semrock). An additional edge filter BLP01 – 325R – 25 (Semrock) was used to cut off scattered radiation from the xenon lamp. The carrier concentration, mobility, and resistivity of the films were measured at room temperature using the van der Pauw four-probe method using an HMS-3000 setup (Ecopia) with a 0.56 T magnet. Figure 1 shows the XRD patterns of HT–ZnO and MOCVD–ZnO thin films, indicating that all ZnO samples exhibit a hexagonal wurtzite structure. The HT–ZnO samples are polycrystalline with a preferred (002) orientation, and the MOCVD–ZnO sample is also polycrystalline with a preferred (110) orientation. Figure 2 shows carrier concentration and mobility in MOCVD–ZnO films annealed for 40 minutes in air, nitrogen, and oil vacuum. Typical room temperature parameters of MOCVD – ZnO films with a thickness of 1.7  $\mu\text{m}$  are the following: free electron concentration  $\sim 5 \cdot 10^{19} \text{ cm}^{-3}$ , carrier mobility 22 – 24  $\text{cm}^2/(\text{V s})$ , resistivity  $\sim 0.005 \text{ Ohm cm}$ . The deviation of these parameters in batches of samples cut from a 100 mm · 100 mm glass substrate did not exceed 10%. The electrical parameters of the film did not change after annealing in air at temperatures below 200°C. At higher annealing temperatures, the carrier concentration gradually decreases, reaching  $\sim 7 \times 10^{17} \text{ cm}^{-3}$  after annealing at 550°C. Likewise, carrier mobility decreases to 0.2 – 0.4  $\text{cm}^2/(\text{V s})$ . It can be concluded that strong scattering occurs at grain boundaries. In addition, carriers are captured by oxygen at grain boundaries, and the concentration of free electrons in the bulk of the ZnO film decreases. This explains the decrease in carrier mobility and concentration.

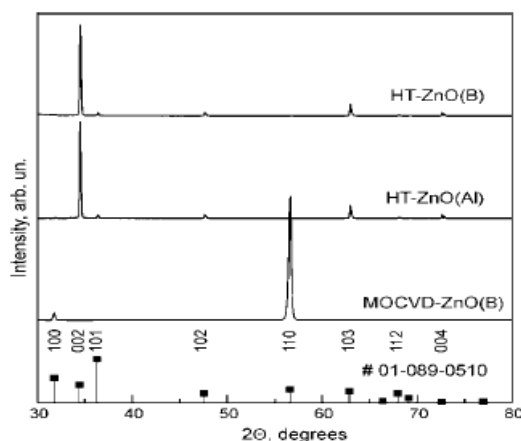
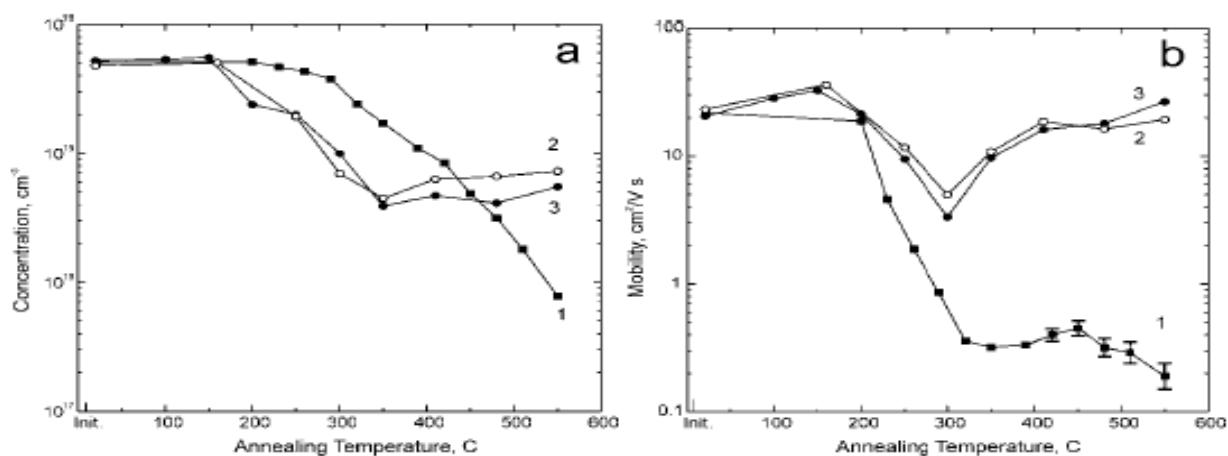


Figure 1 – XRD – samples of HT – ZnO samples doped with a sample of boron or aluminum and MOCVD – ZnO (B). The line diagram at the bottom of the figure shows the

JCPDS #01 map for ZnO with a hexagonal wurtzite-type structure



**Figure 2 – carrier concentration and mobility in MOCVD – ZnO films depending on the annealing temperature in air (1), in a nitrogen atmosphere (2) and in an oil vacuum (3)**

On the contrary, the temperature dependences of carrier concentration and mobility during annealing of MOCVD – ZnO films in vacuum and in nitrogen are significantly different (Figure 48). The mobility increases from 22 – 24 cm<sup>2</sup>/(V s) to 32 – 36 cm<sup>2</sup>/(V s) at annealing temperatures of 150 – 160°C, the carrier concentration also increases slightly. At higher annealing temperatures, the carrier concentration decreases and reaches  $4.8 \times 10^{18}$  cm<sup>-3</sup> upon annealing at 350–550°C, while the carrier mobility is restored to the initial value. This behavior may be due to the fact that annealing in a vacuum and in an inert atmosphere leads to an oxygen deficiency in the surface regions. This promotes the formation of oxygen vacancies and interstitial zinc atoms in ZnO.

Interstitial Zn atoms, which have high mobility and low transport barrier energy, can diffuse into the sample, so they may be responsible for the observed change in electrical properties.

The decrease in electron concentration during annealing may be due to the compensation of boron donors by interstitial zinc atoms. Figure 49a shows the absorption spectra of ZnO samples annealed in oil vacuum. The corresponding energy positions of the Fermi level, calculated from the carrier concentration in these samples, are shown in Figure 3 b as a function of the annealing temperature. It can be seen that at low annealing temperatures (100 and 150°C) absorption increases with increasing photon energies, and at higher annealing temperatures the absorption edge shifts towards low photon energies. These shifts are accompanied by a shift in the position of the Fermi level towards the conduction band, starting with annealing above 150°C, and the energy  $E_g$ , corresponding to optical absorption  $5 \cdot 10^5$  cm<sup>-1</sup>, decreases to 3.31 eV. This can be explained by the formation of oxygen vacancies with states near the bottom of the band gap, and the main contribution to the shift of the optical absorption edge during annealing is associated with the movement of the Fermi level.

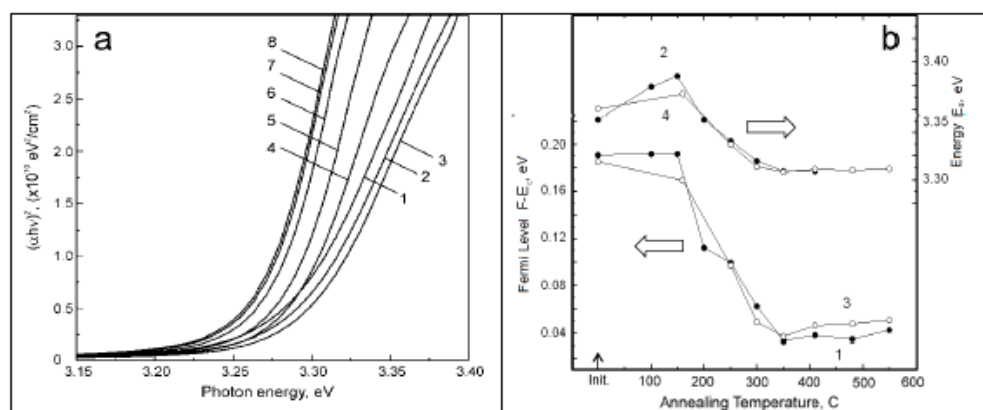


**Figure 3 - (a) Absorption spectra of MOCVD samples - ZnO: initial sample (1) and after annealing in vacuum for 40 minutes at a temperature of 100 (curve 2), 150 (3), 200 (4), 250 (5), 370 (6), 350 (7) and 410oC (8); (b) Dependence of the Fermi level ( $E_F - E_c$ ) on the annealing temperature in ZnO samples during annealing in vacuum (1) and nitrogen (3), calculated from the measured Hall and energy  $E_g$ , which corresponds to an optical absorption of  $5 \cdot 10^5 \text{ cm}^{-1}$ , at annealing in oil vacuum (2) and nitrogen (4)**

Figure 4 shows the effect of annealing on the electrical parameters of two sets of ZnO samples. The first 12 samples were subjected to preliminary annealing in air (curve 1) at 200 – 550°C. Then they were annealed in an oil vacuum for 1 hour at 500°C (curve 2). It can be seen that after annealing, all samples, including the control sample not annealed in air, have approximately the same parameters: mobility  $\sim 23 \text{ cm}^2/(\text{V s})$ , resistivity 0.044 Ohm cm, carrier density about  $6 \cdot 10^{18} \text{ cm}^{-3}$ . Thus, annealing in an oil vacuum eliminates the effect of pre-annealing in air. The second group of 5 samples was annealed in air at 200 – 550°C (the electrical parameters of the samples were the same as for the first group), and then annealed in a high vacuum without oil for 1 hour at 500°C (Figure 4, curve 3). It can be seen that the effect of annealing in an oil-free vacuum in terms of the electrical parameters of the samples differs significantly from annealing in vacuum oil. Then the samples were treated in hydrogen plasma (Figure 4, curve 4), and their electrical parameters returned to the same values as after annealing in an oil vacuum.

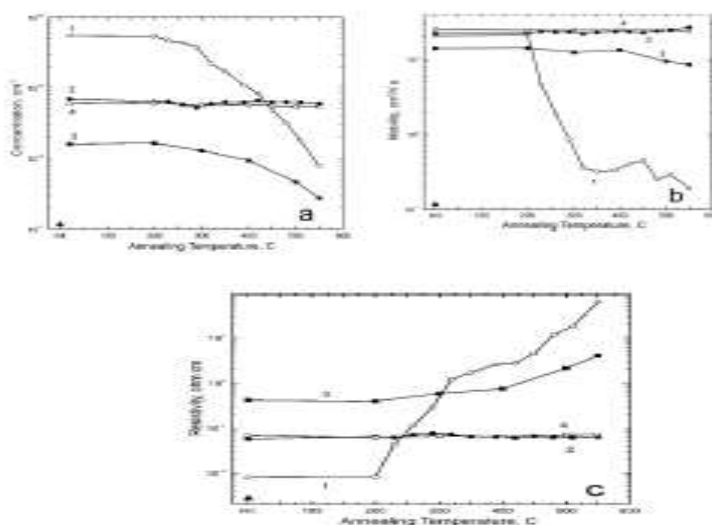


**Figure 4 – Carrier concentration (a), mobility (b) and resistivity (c) in MOCVD – ZnO films, annealed for 40 minutes in air (1) and in vacuum at  $2 \cdot 10^{-2}$  mbar, 1 hour at  $500^{\circ}\text{C}$  (2), ZnO films annealed in air for 30 minutes and in an oil-free vacuum of  $1 \cdot 10^{-5}$  mbar for 1 hour at  $500^{\circ}\text{C}$  (3), followed by treatment in hydrogen plasma for 4 minutes at room temperature (4)**

In both groups, there is an oxygen deficiency on the ZnO surface. However, during oil-free vacuum annealing, excess zinc atoms may evaporate from the surface, and the formation of nonequilibrium interstitial zinc atoms in the surface region becomes difficult. During annealing in an oil vacuum, oil molecules can be absorbed by the catalytically active zinc oxide surface and initiate the carbothermic reduction of zinc oxide. It was previously shown that the exchange of oxygen with the gas phase affects the surface states of ZnO and plays an important role in its electrical conductivity. Thus, in the case of annealing in an oil vacuum, the reduction of ZnO on the surface by organic molecules creates an excess of zinc atoms, which can diffuse into the bulk of the film and recombine with zinc vacancies created under oxygen-enriched conditions.

Probably, the carrier concentration  $(4-8) \cdot 10^{18} \text{ cm}^{-3}$ , achieved by annealing, corresponds to the equilibrium established by the diffusion of zinc from the surface into the bulk. The typical resistivity of the synthesized hydrothermal samples was about  $50 \text{ Ohm cm}$ , so the behavior of the electrical parameters during annealing in air was not studied. Figure 5 shows the change in electrical parameters of HT – ZnO samples doped with boron and aluminum during annealing in vacuum. Films typically show a carrier concentration of about  $2 \times 10^{18} \text{ cm}^{-3}$ , a mobility of  $25 - 27 \text{ cm}^2/\text{V s}$ , and a resistivity of  $0.1 \text{ Ohm cm}$  after annealing at  $450^{\circ}\text{C}$  for 1 hour. It should be noted that undoped HT-ZnO samples also showed similar mobility and resistivity behavior during vacuum annealing, but the low resistivity value after annealing under oxygen deficiency conditions was unstable. The resistance of samples that were stored at room temperature in air for 1 - 2 weeks increased significantly due to exposure to oxygen. In contrast, the electrical parameters of HT – ZnO samples doped with B or Al were stable after annealing (Figure 5). It can be concluded that annealing of HT – ZnO leads to activation of the electrical activity of impurity atoms of boron and aluminum impurities.

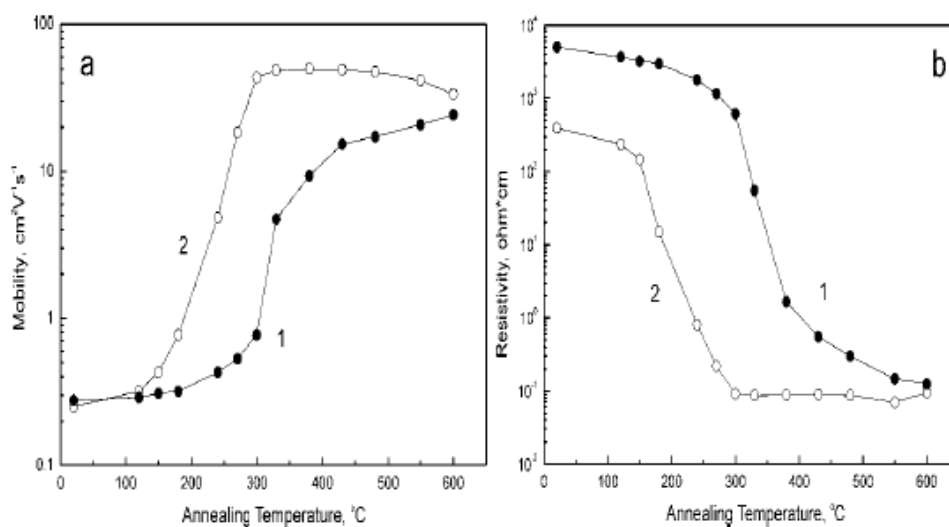


**Figure 5 – Carrier mobility and resistivity in HT – ZnO films doped with B (1) and Al (2) as a function of annealing temperature in an oil vacuum**

Figure 6 shows the PL spectra of HT – ZnO samples annealed in vacuum. The intensity of the band near the absorption edge (NBE) increases after annealing at temperatures of 250 – 400°C and decreases after annealing above 400°C, as in MOCVD – ZnO samples. The dependence of the intensity of the emission band through deep levels (DLE) is non-monotonic upon annealing at 250 – 400°C and decreases upon annealing above 400°C. The intensity first decreases and then increases slightly, and the peak of the band shifts to longer wavelengths. Note that an increase in DLE intensity upon annealing is typical for ZnO samples grown at low temperatures (<200°C).

Hydrogen is known to readily diffuse into ZnO during low temperature plasma treatment (eg, 30 minutes hydrogen plasma treatment at 100oC gives a penetration depth of about 10 microns) and effectively passivates electrically active defects. Hydrogen plasma treatment has a strong effect on the electrical properties of ZnO samples grown by MOCVD and annealed in air. As can be seen from Figure 5, hydrogen treatment completely eliminates scattering at grain boundaries, that is, H – treatment eliminates the effect of oxygen adsorption.

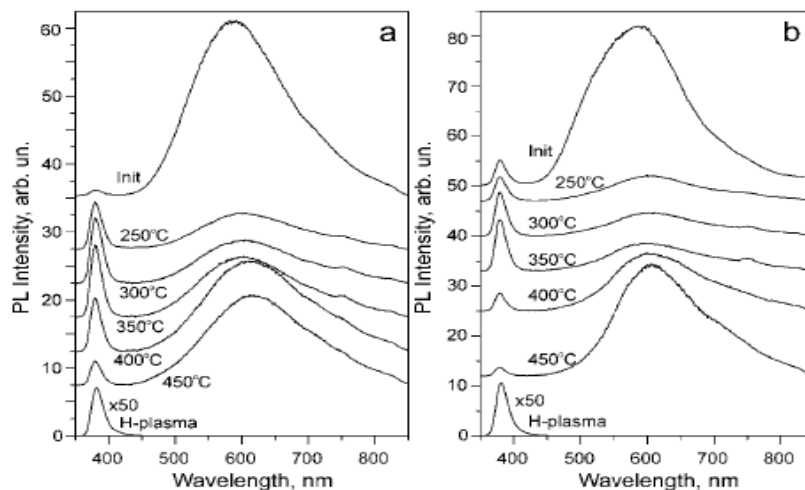


**Figure 6 – PL spectra of initial samples of NT – ZnO films doped with boron (a) and aluminum (b), and samples of NT – ZnO annealed in air. Also shown are the spectra of samples after annealing at 450°C followed by plasma treatment in hydrogen; the intensity of these spectra must be multiplied by 50 for comparison**

Hydrogen treatment was also carried out for ZnO films with a thickness of ~2 microns grown by the hydrothermal method. After a short (4 – 5 minutes) hydrogen plasma treatment at room temperature, the carrier concentration reached  $5.5 \cdot 10^{18} \text{ cm}^{-3}$ , the mobility increased to ~ 30  $\text{cm}^2/\text{V s}$ , and the resistivity was in the range of 0.035 – 0.040  $\text{Om cm}$ . We investigated the effect of hydrogen plasma treatment on the photoluminescence of samples grown by MOCVD and hydrothermal methods. The PL spectra of ZnO samples at room temperature before treatment consisted of a narrow (~0.25 eV) NBE peak at ~380 nm and a broad deep level emission (DLE) band ranging from 450 to 800 nm with a maximum around 500 nm. Typical PL spectra of synthesized ZnO samples, as well as samples annealed at 400°C and treated in hydrogen plasma,

are shown in Figure 7, along with the dependence of the NBE band intensity on the annealing temperature shown in the inset in Figure 7.

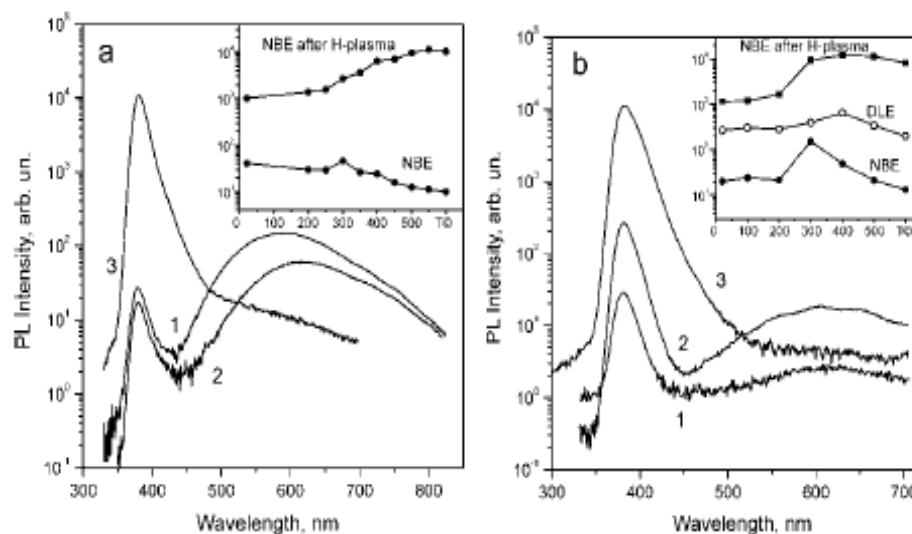


**Figure 7 – PL spectra of samples HT – ZnO (a) and MOCVD – ZnO (b): 1 – initial spectra, 2 – after annealing in air at 400°C for 30 min and 3 – after treatment in hydrogen plasma at room temperature for 4 min. The inset shows the dependence of the intensity of the NBE band on  $T_{\text{revers}}$  in samples annealed in air for 30 minutes at the appropriate annealing temperature and after treating these samples for 4 minutes in hydrogen plasma**

It can be seen that at higher annealing temperatures the NBE intensity increases, passes through a maximum at an annealing temperature of about 300°C, and begins to decrease. At the same time, the DLE intensity begins to increase above 200 – 300°C. This is consistent with the results of the work. Treatment with hydrogen plasma increases the intensity of NBE and leads to the disappearance of the DLE band. Passivation of the DLE strip occurs at room temperature and in a short time. This effect has been noted in a number of studies. The average increase in NBE band intensity after hydrogen plasma treatment was 25 – 35 times in hydrothermal and MOCVD grown samples. The effect of hydrogen plasma treatment was found to depend on the pre-annealing temperature in air, and the intensity of the NBE band increased in pre-annealed samples. The inset in Figure 7 shows that although the intensity of the NBE band changes slightly with increasing annealing temperature, it increases very strongly after hydrogen treatment in both HT-ZnO and MOCVD-ZnO samples. If the PL intensity increases after treatment with hydrogen 50–60 times in the initial samples, then for samples after preliminary annealing the PL intensity increases after hydrogen treatment by three orders of magnitude. Pre-annealing in air has little effect on the intensity of the NBE band at annealing temperatures below 200°C. At higher annealing temperatures, the PL intensity increases, reaching a maximum at 400 – 550°C. In the case of annealing in vacuum and nitrogen, the dependences of the PL intensity are the same and differ from annealing in air. Preliminary annealing already at 100 – 160°C has a significant effect on the dependences. The maximum effect of preliminary annealing in vacuum and nitrogen on the intensity of the NBE band is observed at ~ 250°C, while above 350°C the PL intensity changes slightly.

### Conclusion

Thus, in this work, the electrical properties (concentration and mobility of carriers, resistivity), optical absorption spectra and photoluminescence of polycrystalline ZnO films were studied depending on thermal and plasma treatment. It has been shown that annealing of MOCVD – ZnO films in an oxygen atmosphere leads to a decrease in the concentration of free carriers due to oxygen chemisorption and the formation of depletion layers at grain boundaries. Carrier mobility decreases due to scattering at charged grain boundaries.

The electrical properties of ZnO samples can be significantly restored by subsequent annealing, and the result of recovery annealing depends on the gas atmosphere during annealing.

Annealing in a nitrogen atmosphere, as well as in an oil vacuum of  $2 \cdot 10^{-2}$  mbar, makes it possible to completely restore carrier mobility, and the carrier concentration stabilizes at the level of  $(6 - 8) \cdot 10^{18} \text{ cm}^{-3}$ . On the contrary, annealing in an oil-free vacuum of  $1 \cdot 10^{-5}$  mbar improves the electrical properties only slightly. Short-term treatment in hydrogen plasma dramatically improves the electrical and photoluminescent properties, and the effect of plasma treatment on the PL intensity depends significantly on the pretreatment of MOCVD–ZnO and HT–ZnO films.

Preliminary annealing in vacuum, as well as in an inert atmosphere, leads to a slight increase in the efficiency of hydrogen treatment, however, annealing in an oxidizing atmosphere at 400 - 500°C followed by treatment in hydrogen plasma leads to the highest NBE intensity. A correlation was discovered between the Fermi level and the shift of the optical absorption edge during thermal annealing [6].

### REFERENCES

1. Brinker C.J., Sherer G.W. Sol-Gel Science. The Physics and Chemistry of Sol-Gel Processing. San Diego: Academic Press, 1990.
2. Rani S., Suri P., Shishodia P.K., Mehra R.M. Synthesis of nanocrystalline ZnO powder via sol–gel route for dye-sensitized solar cells // Solar Energy Materials & Solar Cells. 2008. V. 92. P. 1639-1645.
3. Zhang Y.L., Yang Y., Zhao J.H., Tan R.Q., Cui P., Song W.J. Preparation of ZnO nanoparticles by a surfactant-assisted complex sol–gel method using zinc nitrate // J. Sol-Gel Sci Technol. 2009. V. 51. P. 198-203.
4. Chandrasekaran P., Viruthagiri G., Srinivasan N. The effect of various capping agents on the surface modifications of sol–gel synthesised ZnO nanoparticles // Journal of Alloys and Compounds. 2012. V. 540. P. 89-93.
5. Farhadi-Khouzani M., Fereshteh Z., Loghman-Estarki M.R., Razavi R.S. Different morphologies of ZnO nanostructures via polymeric complex sol–gel 102 method: synthesis and characterization // J. Sol-Gel Sci Technol. 2012. V. 64. P. 193-199.
6. Abdullin Kh.A., Gritsenko L.V., Guseinov N.R., Ismailov D.V., Kalkozova Zh.K., Kumekov S.E., Mukash Zh.O., Terukov E.I. Influence of thermal treatment on the optical and electrical properties of ZnO:B thin films // Materials of Fifth European Conference on Crystal Growth (ECCG5). – Bologna; Italy, 2015. – P. 26.